Journal of Materials Chemistry C

Accepted Manuscript

This article can be cited before page numbers have been issued, to do this please use: L. C. Schmidt, V. Edelsztein, C. Spagnuolo, R. E. Galian and P. H. Di Chenna, *J. Mater. Chem. C*, 2016, DOI: 10.1039/C6TC02265K.

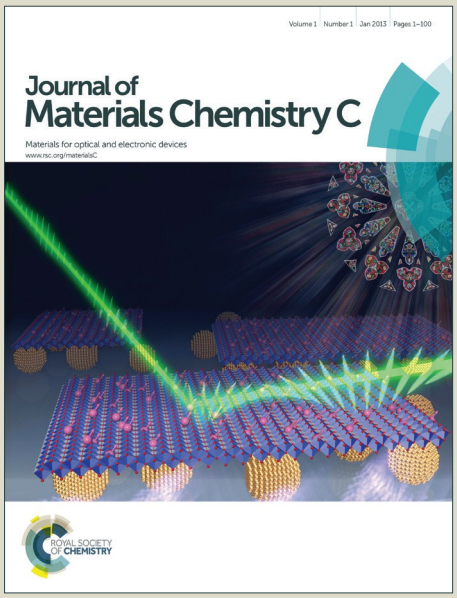

ROYAL SOCIETY OF CHEMISTRY

www.rsc.org/materialsC

DOI: 10.1039/C6TC02265K

Journal Name

ARTICLE

Light-responsive hybrid material based on luminescent core-shell quantum dots and steroidal organogel

Received 00th January 20xx,
Accepted 00th January 20xx

DOI: 10.1039/x0xx00000x

www.rsc.org/

L. C. Schmidt,[a] V. C. Edelsztein,[b] C. C. Spagnuolo,[c] P. H. Di Chenna[b*] and R. E. Galian[d*]

We report the synthesis of a smart novel hybrid with reversible photoswitchable luminescence properties modulated by light. Combination of a low molecular weight organgelator (LMOG) and CdSe/ZnS core-shell semiconductor nanoparticles capped with trioctylphosphine oxide ligands produces a luminescent, stable and transparent material. Modulation of the luminescence properties was succesfully achieved using a diarylethene photochromic compound, with good resistance to fatigue ca. 22 cycles. Interestingly, the morphology of the organogel fibers was preserved in the hybrid, while a partial luminescent quenching of the nanoparticle was observed. This material could have implication for on-and-off photoswitching applications.

1. Introduction

Semiconductor nanoparticles, usually known as quantum dots (QDs), are colloidal inorganic particles of a few nanometers in diameter.[1] To date QDs have been widely used in many areas such as biology, analytical and material chemistry due to their particular size-dependent optical properties, such as broad absorption spectra and very narrow emission spectra.[2-6] They are usually composed of a luminescent core, CdSe or CdTe. The presence of an inorganic shell with a higher band gap than the core (ZnS, CdS, or ZnSe) can properly passivate the surface defects, resulting in an improvement of the quantum yield and photostability. Moreover, the attachment of specific ligands on their surface strongly affects their luminescent properties also providing them with colloidal stability in different media.[7]

Over the last decade the integration of nanoparticles within unconventional microenvironments, such as gels, has emerged as an original area of research.[8] This approach is relevant not only for the design of functional materials, but also for understanding the properties that may arise from the interactions within the components of the hybrid composite. Compared to polymeric gels, low molecular weight organic gelators (LMOGs) show the higher level of innovation in this area by means of a defined mode of self-assembly and the reversibility of their self-assembled fibrillar network (SAFIN). Their network structures are held together by reversible noncovalent interactions such as hydrogen bonding, π–π stacking, etc.[8-11]

Nanoparticles–organogel systems based on LMOGs also allow the design of the material's internal structure easily by specific structural modifications of the LMOG. An example of CdSe/ZnS core-shell QDs incorporation in a pseudopeptidic macrocyclic compound has been recently reported for sensing applications towards nitric oxide.[12] Using the same LMOG results in a symbiotic effect between QDs and the LMOG, producing an enhancement of the CdSe luminescence (ca. 500 %), a reduction of the critical gelation concentration and preserving the supramolecular organization of the internal fibrillar network.[13] However, fluorescence modulation studies were not carried out in those studies.

In this work, a non-cholesteryl steroid organogel (OG1) was chosen to prepare a transparent and stable hybrid material in the presence of different kind of semiconductor nanoparticles, capped with long chain amines or trioctylphosphine oxides as ligands (Figure 1).

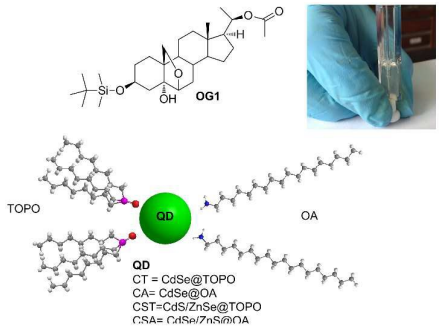

[a] INFIQC-CONICET, Departamento de Química Orgánica, Facultad de Ciencias Químicas, Universidad Nacional de Córdoba, 5000 Córdoba, Argentina.
[b] UMYMFOR-CONICET, Departamento de Química Orgánica, Facultad de Ciencias Exactas y Naturales, Universidad de Buenos Aires, Ciudad Universitaria, C1428EGA, Buenos Aires, Argentina. E-mail: dichenna@qo.fcen.uba.ar
[c] CIHIDECAR-CONICET, Departamento de Química Orgánica, Facultad de Ciencias Exactas y Naturales, Universidad de Buenos Aires, Ciudad Universitaria, C1428EGA, Buenos Aires, Argentina.
[d] ICMOL, Universidad de Valencia, Catedrático José Beltrán 2, 46980, Paterna, Valencia, España. E-mail: raquel.galian@uv.es

Electronic Supplementary Information (ESI) available: Additional absorption, emission, NMR Spectra and tables. See DOI: 10.1039/x0xx00000x

View Article Online
DOI: 10.1039/C6TC02265K

Figure 1: Scheme of the LMOG (OG1) and QDs capped with trioctylphosphine oxide (TOPO) and octadecylamine (OA). Picture of the organogel CST-OG1.

The non-cholesteryl steroid organogel has been previously combined with an organic fluorophore such as tetraphenolxylated perylene diimide.[14] In this case, the dye doped organogel was used as template for the growing of silica nanoparticles. The use of inorganic fluorophores like quantum dots could improve the potential application of the luminescent organogel due to their higher luminescence quantum yield and longer fluorescence lifetimes than organic fluorophores.

Electroluminescent devices, sensors, and informational displays require smart materials, which have the ability to switch their photoluminescent properties in response to external stimuli. It was envisaged that the incorporation of a photochromic activator/quencher, such as spiropyran and diarylethene derivatives could be used as an effective methodology to modulate the light-emitting property of QDs. Attachment of those photochromic compounds to the semiconductor nanoparticle surface has been carried out by different strategies i) using a biotinylated diheteroarylethene derivative bounded to the quantum dots bearing a conjugated streptavidin[15] ii) linking covalently the diarylethene to an amphiphilic polymer that self-assembles with the lipophilic chains ligands of hydrophobic core-shell CdSe/ZnS QDs[16] and iii) mixing a thiolated spiropyran with core-shell QDs. [17]

In particular, diarylethene (DAE) has been used as photochromic compound embedded into the fluorophore-organogel system (perylene compound-OG1), preserving its ON-OFF properties.[14] Also, it has been combined with organic semiconductor material such as *n*-type fullerene derivative to construct photoswitchable hybrid thin-film transistors. Engineering the diarylethenes' LUMO, which act as an intra-gap state controlled by a different wavelength in the UV or in the visible range, a good control over the device output current was achieved.[18]

The results reported herein, combine the intrinsic properties of the luminescent QDs and the organogelator OG1 to obtain a luminescent photoswitchable QDs-organogel hybrid material, modulated by an embedded photochromic diarylethene. This novel, thermoreversible and luminescent QD-organogel hybrid increases the attractiveness of these materials and offers an effective strategy to modulate the light-emitting property in a predictable fashion.

2. Experimental Section

Materials and methods

All starting materials were purchased from Sigma-Aldrich and were used as received. Solvents were dried and purified by standard methods prior to use. The organogelator pregnane steroid (OG1) and the diarylethene photochromic compound (DAE) were synthesized and characterized following a standard procedures.[19-20]

Synthesis of QDs

Quantum dots were synthesized following previous methodology with some modification. CdSe core QD capped with trioctylphosphine oxide (CT) and octadecylamine (CA) and the CdSe/ZnS core−shell capped with trioctylphosphine oxide (CST) and octadecylamine (CSA), as organic ligands were obtained.

The mixture of CdO (102 mg), TDPA (446 mg), and trioctylphosphine oxide (7.560 g) was heated at 300 °C under nitrogen until a clear solution was obtained. Then, the temperature was lowered to 220 °C and a solution of Se in trioctylphosphine (82 mg in 4.8 mL) was added and maintained during 5 min.

Then, an aliquot of 7 mL was taken and precipitated in cold ethanol, centrifuged three times (8000 rpm), and redissolved in toluene to yield CT-QDs.

The rest of the above-mentioned mixture was cooled to 120 °C and a solution of $ZnEt_2$ (197 mg) and $(TMS)_2S$ (250 mg) in trioctylphosphine (5 mL) was added dropwise. After addition, the mixture was maintained at 70 °C for 24 h. After cooling down to room temperature, ethanol was added and the resulting precipitate was separated by centrifugation and then dissolved in hexane to yield CST QDs.

The CT QDs and CST QDs were used to obtain CdSe core capped with octadecylamine and the CSA-QDs, respectively. The ligand exchange reaction was made in toluene under nitrogen atmosphere during 48 h, using an amine: QD ratio of 5000 : 1. The resulting nanoparticles were precipitated, centrifuged, and washed with ethanol and redissolved in toluene to yield CA-QDs and CSA-QDs.

Preparation of QD-OG1

A mixture of the gelator OG1 (6 mg, 1 % w/v), and the QD (30 μL of 1x 10^{-5} M to get a final concentration of 0.5 μM,) were added in a closed flask using *n*-hexane (570 μL) as solvent. The mixture was heated up to 70 ºC, under shaking until the solid was dissolved. Then, the hot solution was transferred into a quartz-cuvette and cooled down to room temperature to form a stable and transparent gel QD-OG1.

Fluorescence Measurements

For the analysis of the modulation of the fluorescence emission of CST by the DAE in the organogel, a mixture of the organogelator OG1 (5 mg, 1 wt %), DAE (0.7 mg; final concentration: 2.5 mM), CST (25 μL from a 22.8 μM solution; final concentration: 1.14 μM) and *n*-hexane (475 μL), in a closed flask was heated and shaken until the solid was dissolved. Then, the hot solution was placed in a cuvette and cooled to room temperature to form a stable gel.

Corrected fluorescence emission spectra were obtained on a Cary Eclipse spectrophotometer equipped with two Czerny-Turner monochromators and a 15 W Xenon pulse lamp (pulse width: 2-3 us, power: 60-75 kW). When temperature control was necessary, the cell was thermostated using the Thermal Application of the ADL software. Fluorescence lifetimes were determined by time-correlated single photon counting (TCSPC) in a HORIBA Jobin Yvon IBH 5000U apparatus. The excitation source was a NanoLED 457 nm and detection was performed with a TBX-PS detector with a band pass emission filter

View Article Online
DOI: 10.1039/C6TC02265K

centered at 540 nm. Fluorescence decays were recorded using an impulse repetition rate in reverse TAC mode >100 kHz. Acquisition was terminated when the peak signal reached 10,000 counts. DAS6v6.2 decay analysis software or Nonlinear ModelFit routine of Mathematica (Wolfram Research) were used for lifetime calculations. The quality of fit was judged by the value of χ^2 and visual inspection of the residuals. A diluted solution of Ludox was used for prompt excitation.

The light source for the photochromic switching was a Lumatec Superlite SUV-DC-P irradiator equipped with a 200 W DC Super Pressure Short Arc Mercury lamp, time selector for irradiation and fiber optic coupled output. Two filters were used for fine wavelength selection. DAE closed form was reached using a UV filter (340 nm) and an ambar filter (590 nm) for the reverse opening reaction. Light source power at 366 nm was approximately 154 μW and 9 mW at 547 nm.

High resolution transmission electron microscopy (HRTEM) and Transmission electron microscopy (TEM)

Microscopy images were carried out by using a Field Emission Gun (FEG) TECNAI G2 F20 microscope operated at 200 kV and a TEM Philips EM 301 for the HRTEM and TEM images, respectively. HRTEM samples were prepared from a toluene dispersion of the NPs, and a few drops of the resulting suspension were deposited onto a carbon film supported on a copper grid, which was subsequently dried. TEM samples of gels and hybrids in *n*-hexane were prepared leaning the carbon film-copper grids onto the surface of the organogel material for 2 seconds, and then were subsequently dried.

Infrared measurements (ATR)

Infrared ATR measurements of CST and CST-OG1 were performed on a Nicolet iS50 ATR FT-IR spectrometer.

Nuclear magnetic resonance (NMR)

^{1}H and ^{31}P NMR spectra were measured in a Bruker Avance II 500 (500.13 and 202.45 MHz) NMR spectrometer in deuterated chloroform.

3. Results and discussion

The role of the none-cholesteryl steroid organogelator (OG1**,** 3ß-tert-butyldimethylsilyloxy-20-acetyloxy-5α-hydroxy-6,19-epoxy-pregnane) on the optical properties of core (CdSe) and core-shell (CdSe/ZnS) quantum dots, capped with trioctylphosphine oxide or octadecylamine, was evaluated (Figure 1).

This organogelator compound has been reported to form transparent organogels from *n*-hexane and acetone with a minimum concentration for gelation (MCG) of 0.2 wt.% at 24°C and 3.1 wt.% at 5°C, respectively, but no gelation was observed in chlorinated solvents such as chloroform. OG1 was synthesized and characterized following a previously reported procedure. [19]

Quantum dots (QDs) were synthesized using previous methodologies but with some modification (see experimental section for details). A key point during the synthesis of QDs was to obtain nanoparticles with similar core size and optical properties but different organic capping. The CdSe core QD capped with trioctylphosphine oxide (TOPO, CT) and octadecylamine (OA, CA) as organic ligands were used as seed for the synthesis of CdSe/ZnS core-shell nanoparticles, to get the CST and CSA, respectively. All QDs were soluble in toluene, chloroform, dichloromethane and *n*-hexane.

The optical properties of all synthesized nanoparticles are summarized in table S1. They have similar maximum in the absorption spectra between 513 and 519 nm (Figure S1-S2) and the calculated core diameters were *ca.* 2.5 nm.

Regarding to the emissive properties, the fluorescence maxima were observed between 523 and 532 nm depending on the core (Figure S1) or core-shell (Figure S2) QDs and the fluorescence quantum yield was lower than 10 % for core QDs and higher than 45 % for the core-shell QDs, in agreement with a good inorganic passivation (ZnS shell). The total size of the core-shell nanoparticle was calculated by microscopy techniques, and the thickness of the shell obtained was 0.7 and 1.1 nm for CST and CSA, respectively. Moreover, high resolution transmission electron microscopy (HRTEM) images showed a good monodispersity, crystallinity and quality of the nanoparticles (Figure S3). The monodispersity of the samples was also confirmed by the small full width at half maximum (FWHM) of 28-29 nm (Table S1).

Synthesis and optical properties of the hybrid organogels

In order to obtain the luminescent organogel, a mixture of the gelator OG1 (6 mg, 1 wt.%), and the QD (0.5 μM,) were added in a closed flask using *n*-hexane as solvent (see experimental section). The mixture was heated up to 70 ºC, under shaking until the solid was dissolved. Then, the hot solution was transferred into a quartz-cuvette and cooled down to room temperature to form a stable and transparent gel QD-OG1 (Figure 1).

In the case of core QDs-OG1 a drastic fluorescence quenching of the QDs was observed upon formation of the gel, a total quenching for CT and a decrease of 74 % for CA (Figure 2, Table S2). However, in the case of core-shell QDs-OG1 similar decrease was observed for CSA (75 %) and a lower fluorescence quenching for CST (53%). These results seem to indicate the key role of the organic ligands and the shell on the interaction nanoparticle-organogel. Octadecylamine, a long chain amine ligand, produced the same fluorescence quenching whether the nanoparticles were a core or a core-shell QDs. However, the bulky ligand TOPO seems to strongly interact with the organogel causing a different fluorescence quenching efficiency for core and core-shell QDs, as will be discussed in the following sections.

The maximum in the emission spectra was maintained in the gel medium for all hybrids.

In addition, time resolved fluorescence studies were carried out to determine the lifetime of the QDs in solution and in the organogel QDs-OG1. A clear reduction of the average lifetime of the QDs was observed in all cases in a similar trend than the reduction of the fluorescence quantum yield (Table S2).

View Article Online
DOI: 10.1039/C6TC02265K

Interestingly, when a solution of OG1 in *n*-hexane with a concentration below the MCG was used (0.1 wt.%), the luminescent properties of the CST (Φ = 55 %, τ_{av}= 69.6 ns, were slightly reduced (Φ = 53 %, τ_{av}= 64 ns, Figure S4). This behaviour could indicate an interaction of the OG1 with the QDs even before the formation of the CST-OG1 hybrid at 1 wt.% (Φ = 25.7 %, τ_{av}= 45.2 ns, Figure S4). In order to further modulate the luminescent properties of the hybrid material, it is necessary to preserve as much as possible the luminescence properties of the system, so the following experiments were carried out with CST-OG1 hybrid, which showed nice emissive properties and fluorescence lifetime better than many organic fluorophores.

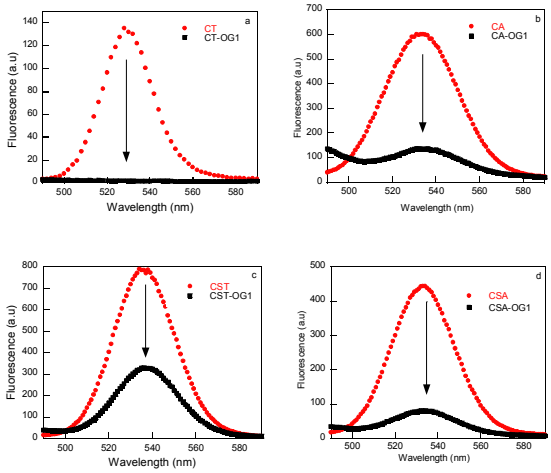

Figure 2: Fluorescence of QDs (0.5 μM) in solution and in the organogel OG1 (1% w/w) in *n*-hexane for the a) CT, b) CA, c) CST and d) CSA.

Steady- state and time-resolved studies

The effect of increasing concentrations of the OG1 on the emission of CST was analyzed in the range of 0.5 to 3 wt.%, using chloroform as solvent, to avoid the formation of the organogel (Figure 3). As the concentration of OG1 was increased, the emission decreased, keeping the maximum at 537 nm. A linear Stern-Volmer plot (F/F_0 vs. [Q], Figure 3) was obtained according to equation 1, where F and F_0 correspond to the fluorescence emission at 537 nm in the presence and in the absence of quencher, respectively, K_{SV} is the Stern Volmer quenching constant and [Q] the quencher concentration.[21]

$$\frac{F_0}{F} = 1 + K_{SV}[Q] \quad \text{Equation 1}$$

The quenching constant (K_{SV}) value obtained was of 23.6 M^{-1}. Time resolved measurements were done in order to get more information about the fluorescence quenching mechanism (Figure S5). The fluorescence decays were fitted to four exponential functions in order to get low χ^2 and weighted residuals values. This behaviour is in agreement with the complex multiexponential decays reported for QDs and are related to the combination of surface chemistry effects and to the different response of individual nanoparticles present in the batch.[22-25] In order to easily compare the lifetimes of QDs in the organogel medium the average lifetime (τ_{av}) was calculated following Equation 2, where τ_i represents the luminescence decay times and α_i represents the amplitudes of the components.[26] Luminescent average lifetimes of CST at increasing concentration of OG1 are summarized in Table S3.

$$\tau_{av} = \frac{\sum \alpha_i.\tau_i^2}{\sum \alpha_i.\tau_i} \quad \text{Equation 2}$$

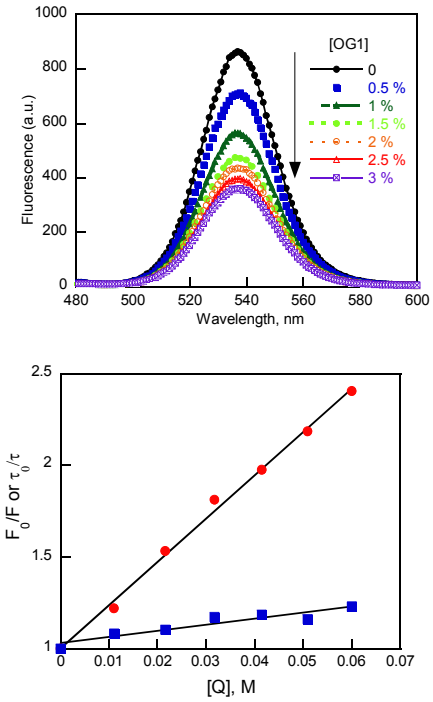

Figure 3: a) Fluorescence spectra and b) Stern-Volmer plot of CST in the presence of different amounts of OG1 in chloroform, fluorescence intensity (●) and fluorescence lifetime (■).

The average lifetime of the CST was slowly reduced with a linear Stern-Volmer constant K_{SV}= 3.34 M^{-1} and a dynamic quenching constant K_q of 0.41 x 10^9 $M^{-1}.s^{-1}$ (τ_{av} was the average lifetime obtained from equation 2 at different quencher concentrations and τ_{av0} was the average lifetime in the absence of quencher with a value of 58.1 ns).[21] These values are indicative of the small contribution of the dynamic quenching to the whole process (Figure 3).

$$\frac{\tau_{av0}}{\tau_{av}} = 1 + \tau_{av0}.k_q[Q] \quad \text{Equation 3}$$

A close inspection of the radiative (k_r) and none-radiative (K_{nr}) constants calculated according to the literature (Table S3 and equation S1 and S2)[21] shows a higher increase of the ratio K_{nr}/K_{nr0} compare to the decrease of the K_r/K_{r0}, as the concentration of the OG1 increases (Figure S6). This behaviour could be related to a reorganization of the ligands or the formation of new defects on the quantum dots surface, as indicates the increase of the K_{nr}. It is well known that surface defects can reduce the recombination of the electron-hole pair

View Article Online
DOI: 10.1039/C6TC02265K

by trapping an electron or hole reducing the luminescent properties of QDs. These results indicate that the main contribution to the fluorescence quenching mechanism is static and can be assigned to a strong interaction between OG1 and the nanoparticle surface in the gel media.

Characterization of the hybrid CST-OG1

The synthesized hybrid CST-OG1 was characterized using different techniques such as a high-resolution transmission electron microscopy (HRTEM), nuclear magnetic resonance (NMR) of proton and phosphorous and infrared spectroscopy (FT-IR).

Microscopy images were taken for the hybrid CST-OG1 and compared with the OG1 and CST nanoparticles. Interesting, the QDs can be clearly observed on the organogel network, which preserve the OG1 morphology (Figure 4).

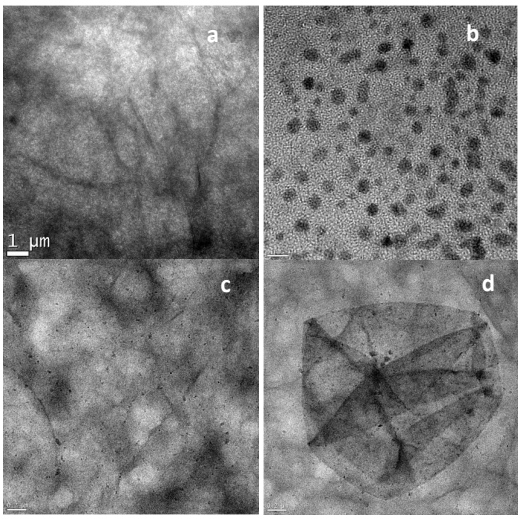

Figure 4: HRTEM images of OG1 (a, 1 µm), CST (b, 5 nm) and CST-OG1 (c,d 0.2 µm)

In order to better understand the interaction between the CST and OG1, a detailed study was done using ^{1}H-NMR and ^{31}P-NMR techniques. These experiments were performed on deuterated chloroform to follow the effect of OG1 in a solvent where the organogel is not formed. Briefly, to an NMR tube containing 0.6 mL of CST (76 µM) in $CDCl_3$ increasing amounts of OG1 (8-51 mM) were added and ^{1}H-NMR and ^{31}P-NMR spectra were collected (Figure 5 and 6). Before each NMR experiment the solutions were allowed to stabilize during 5 minutes.

Although the ^{1}H-NMR signals of the organogelator in the CST+OG1 mixture did not show any shift, a considerable broadening of the signals was observed together with a loss of the resolution, in particular for the protons H-19, H-20, H-3 and H-6 (Figure 5). It could indicate an interaction of the OG1 carbonyl group of the ester with the nanoparticle surface and OH group. See Figure S7 and S8 for the full scale spectra of pure OG1 and CST+OG1 mixture, respectively. This noticeable broadening is in agreement with those observed for other organic molecules interacting with the surface of a core-shell QDs structure.[27-29 28]

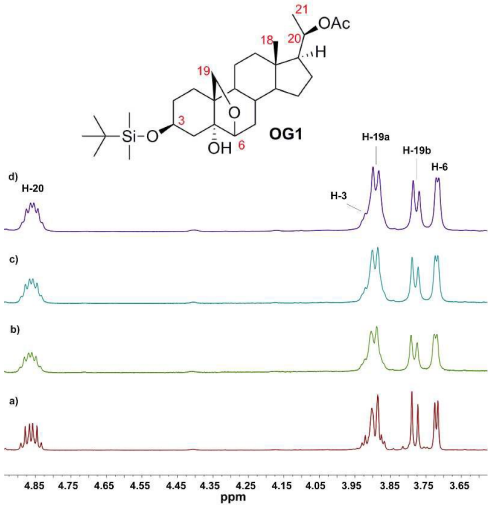

Figure 5: ^{1}H-NMR (500 MHz, $CDCl_3$) zoom 5.0 - 3.6 ppm a) OG1 (8 mM) b) QDOT-CST (76 µM) +**OG1** (8 mM) c) QDO-CST (76 µM) + **OG1** (23 mM) d) QDOT-CST (76 µM) + **OG1** (51 mM)

In the case of ^{31}P-NMR spectra, the analysis of an expansion in the range 47-50 ppm showed a slight but clear shift towards lower field of the phosphorous signal of TOPO in the CST, from 48.66 ppm for pure CST to 48.81 ppm at the higher concentration of OG1 used (Δppm= 0.15). Interestingly a narrowing of the signal could be observed to the naked eye. The full width at half maximum (FWHM) was measured finding a value of 38.5 Hz for TOPO in CST (Figure 6a) and 22.4 Hz for TOPO in the CST+OG1 mixture (ΔHz= 16.1) at the higher concentration of OG1 (51 mM) used (Figure 6d).

It is noteworthy that the ^{31}P NMR signal at 48.69 ppm (Figure 6) did not show any change during the addition of OG1, so it can be used as internal reference. The observation of this two type of signals could be indicative of the presence of two kind of TOPO on the CST QD, one TOPO strongly interacting with the surface (broad, centered at 48.66 ppm) and some TOPO encapsulated close to the surface (narrow at 48.69 ppm).

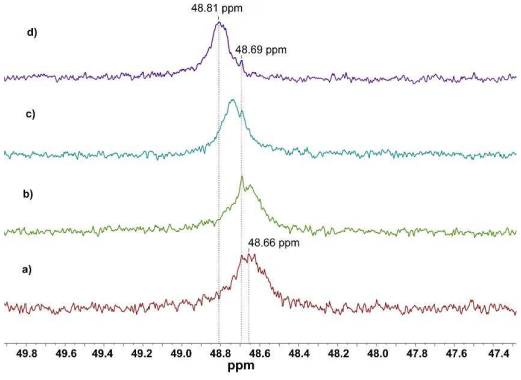

Figure 6: ^{31}P-NMR (202.5 MHz, $CDCl_3$) a) CST (76 µM) FWHM: 38.5Hz b) CST+OG1 (8 mM) FWHM: 27.4Hz c) CST + OG1 (23 mM) FWHM: 25.9Hz d) CST + OG1 (51 mM) FWHM: 22.4Hz.

View Article Online
DOI: 10.1039/C6TC02265K

A control experiment performed on a solution of free TOPO (20 mM) in the presence of OG1 (20 mM) in deuterated chloroform (Figure S9) produced a similar shift from 48.59 ppm towards 48.75 ppm (Δppm= 0.16), but just a slight narrowing of the signal was obtained from 6.3 Hz for free TOPO towards 3.2 Hz for the TOPO+OG1 mixture (ΔHz= 3.1).
These changes observed in the ^{1}H-NMR signals of OG1 and ^{31}P-NMR signals for TOPO in CST are indicative of an interaction between the gelator and the phosphine oxide group of the capping ligand. This is also observed for the intermolecular interaction of free TOPO and OG1 in concordance with some reported studies for other macrocyclic organogels-QDs system.[13]

To get a better inside into the interactions between the nanoparcticles and organogelator molecules Infrared-spectra (ATR) were obtained for CST-OG1 and were compared with those of OG1, TOPO and CST. The only differences observed were a slight shifting for the O-H and the C=O stretching bands on OG1 from 3426.7 and 1729.9 cm^{-1} to 3420.7 and 1728.9 cm^{-1} in CST-OG1, respectively. Besides, IR spectra of a mixture of OG1 and TOPO showed a clear difference for the O-H stretching band. In presence of TOPO a clear broadening of the signal at 3426 cm^{-1} appeared together with a wide shoulder at 3300 cm^{-1} that accounts for interaction of OG1 with the ligand through hydrogen bond (Figure S10-S11). These interactions, revealed by FT-IR and NMR spectroscopy, can be responsible of the fluorescence quenching observed for the CST in the organogel medium and the alteration of QDs surface.

Effect of temperature in the fluorescence of CST-OG1

The effect of the temperature on the luminescent properties of the CST-OG1 hybrid was analysed in the range 0-75 ºC, at intervals of 10 ºC. Fluorescence intensity was preserved in the temperature range 0-30ºC, but above this value the luminescence decreased reaching a reduction of 52 % at 75ºC (Figure S12). This behaviour is in agreement with the fluorescence quenching of the nanoparticle by OG1 in solution. The gel-sol transition temperature (Tg) of the hybrid was estimated to be 56^{o}C from the inflection point of the curve (Figure S12) which is in excellent accordance with the value previously reported for an organogel of OG1 in *n*-hexane at the same concentration using Differential Scanning Calorimetry (54^{o}C, 1.0 wt.%).[19] Moreover, the Tg values of the CST-OG1 hybrid gel and OG1 gel were also measured simultaneously using the inverted tube method with the same concentration of OG1 (in this experiment 1.3 wt.%). The Tg on the organogel hybrid CST-OG1 (62-68 ºC) was similar to that of the *n*-hexane gel of OG1 (64-66º C), this together with the preserved morphology of the structure observed by SEM are clear evidence that the nanoparticles does not affect the self-assembly of OG1 as it was also observed for this organogelator doped with an organic fluorophore.[14] It is also noteworthy that total recovery of the CST fluorescence is obtained when the temperature reaches 20º, indicating a good thermoreversibility of the system that can be done at least 5 times.

Stability of the CST-OG1

The stability of the hybrid CST-OG1 organogel (1.14 μM CST, 1% w/v OG1 in *n*-hexane), in the presence of a small amount of solvents such as acetone, water and *n*-hexane was evaluated. The luminescent properties of the hybrid were taken every minute after the addition of the solvents on the organogel surface. Only in the case of acetone (50 μL) the luminescence of the CST was recovered (Figure S13). Diffusion of water and acetone into the hybrid material caused the disruption of the self-assembled network of OG1. In the case of water a quenching of the fluorescence of CST was obtained (Figure S13b). Similar breaking down of CdSe/ZnS QDs in gel based on polymers has been reported in the presence of water, due to a competitive hydrogen bound formation between water molecules and amide or amine groups of the polymer compared to the intermolecular hydrogen bound in the polymer structure (amide-amine).[30] In the case of acetone an enhancement of the luminescence *ca*. 40 % was observed related to the delivery of the nanoparticle to the solution (Figure S13a). The luminescence of the CST-OG1 in the presence of the similar amount of *n*-hexane was analysed during 100 minutes and no change was observed, indicating that the CST-OG1 hybrid maintained their internal structure (Figure S13c).
These preliminary results indicates that the diffusion of small polar molecules such as acetone can lead to the recovery of the QDs fluorescence by disruption of the 3D self-assembled fibrillar network present on the organogel hybrid with subsequent liberation of QDs to the medium.

Modulation of the luminescent properties of the hybrid by DAE

Photocromic properties of DAE are well known, under UV light irradiation the open form (colourless) photoconverts to the close form (purple colour, λ_{max}= 550 nm). The close form can be reverted to the open form by visible irradiation. The on-off function of different fluorophores arises from the photoisomerization capabilities of this diarylethene.
Interesting, this properties were preserved in the organogel hybrid as can be observed in Figure 7.

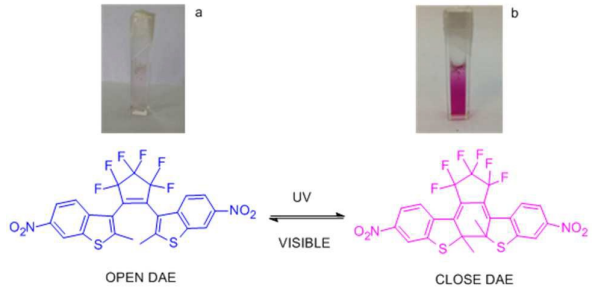

Figure 7: Scheme and pictures of DAE photoswitching in the CST-OG1 hybrid, a) open form of DAE and b) close form of DAE.

View Article Online
DOI: 10.1039/C6TC02265K

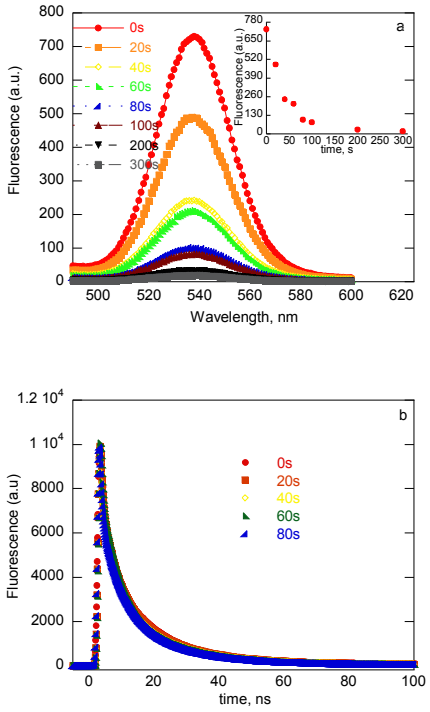

Figure 8: a) Fluorescence emission spectra and b) fluorescence lifetime of CST-OG1 (λ_{exc} = 457 nm) in the presence of DAE (2.5 mM), upon irradiation with UV lamps. Fluorescence loss efficiency = 97 % in the CST-OG1. Inset: fluorescence intensity at 537 nm vs. irradiation time.

In order to check the light-responsive behaviour of the hybrid material, modulation of the CST-OG1 and CST emission by DAE (2.5 mM) was studied. The samples were irradiated with UV-lamps for 320 seconds and fluorescence spectra and decays were taken every 20 seconds as shown in Figures 8 and S14 for CST-OG1 and CST, respectively.

The emission intensity of the CST can be gradually switched off by increasing the irradiation time with UV-light reaching a quenching efficiency of 97-98 % in both systems (Figure 8a and S14a).

To go further in the understanding of this quenching mechanism, we performed the time-resolved experiments. As the lifetime of QDs did not change with the irradiation time (i.e. increasing the concentration of closed form of DAE, Figure 8b and S14b) we proposed that the quenching mechanism observed in the stationary state is due to energy transfer from the nanoparticle toward the closed form of the acceptor through the so-called trivial mechanism.[21] It is in agreement with the mechanism proposed for other photoswitchable CdSe/ZnS quantum dots.[15-16, 31]

In addition the absorption spectra of all possible organic molecules present in the system (TOPO, DAE, OG1) were added in Figure S15, ESI. Only the closed form of DAE presents an absorption band at around 550 nm that overlaps with the emission of QDs.

Once the OFF state was reached, samples were irradiated with visible-light for 30 minutes to recover the original emission intensity. This UV-Vis irradiation cycle between the two isomers of the DAE compound was repeated more than 20 times rendering reproducible ON-OFF states, indicating the low fatigue of the system under study (Figure 9). They are especially high-rated photochromic switches due to their high resistance to fatigue when subjected to large ON-OFF cycles.[32-34]

The excellent durability of the hybrid was demonstrated by analyzing the morphology of the organogel before and after photoswitching experiments, in the presence of DAE, by microscopy techniques. The TEM images showed that the internal fibrillar network of OG1 is preserved after one ON-OFF cycle and have the same morphology than the control experiments, OG1 irradiated under the same experimental conditions (Figure S16) and OG1 without irradiation (Figure 4a).

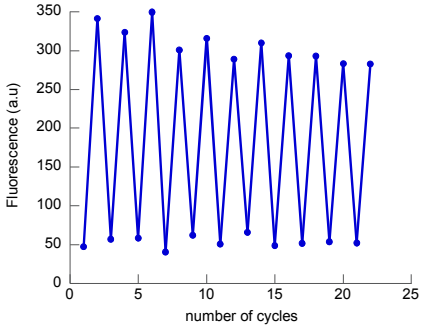

Figure 9: Modulation of the fluorescence of CST-OG1 from *n*-hexane through UV-Vis irradiation cycles (30 min vis – 10 min UV) between the DAE closed and open form.

Photostability of CST in CST-OG1 hybrid in the presence of DAE forms

For the analysis of the photostability of the CST in the CST-OG1 hybrid in the presence of both forms of DAE, a mixture of the gelator OG1 (5 mg, 1 % w/v), DAE (2.5 mM), CST (1.14 μM) and *n*-hexane, in a closed flask were heated and shaken until the solid was dissolved. Then, the hot solution was placed in a cuvette and cooled to room temperature to form a stable gel.

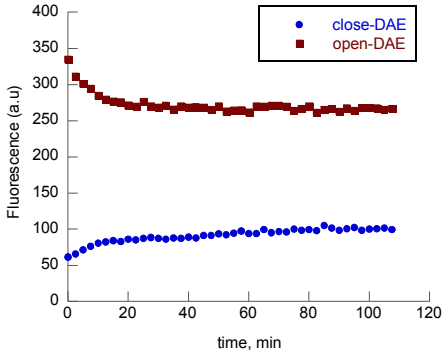

Figure 10: Photostability of **CST** in the CST-OG1 from *n*-hexane for the DAE open (red) and close form (blue).

DOI: 10.1039/C6TC02265K

For the open form of the DAE, the sample was irradiated with visible light for 30 minutes and fluorescence emission spectra were taken every 2.5 minutes for 110 minutes. In the case of the close form of the DAE, the sample was irradiated with UV light for 10 minutes and fluorescence emission spectra were taken every 2.5 minutes during 2 hours (Figure 10). It is noteworthy that in both case after 10 minutes the luminescence of the CST in CST-OG1 was practically constant indicating the good photostability of the CST in the system.

4. Conclusions

The hybrid QD-organogel system object of this work is a well-characterized example of an integrated multifunctional nanosystem that combines luminescence from the inorganic nanoparticle, a stable organogel medium by OG1 and photochromic activity by the diarylethene compound. A stable, luminescent and photoswitchable organogel was successfully obtained with excellent optical response. Thermal and morphological studies indicated that the presence of the nanoparticles does not affect the self-assembly of the organogelator molecules and therefore neither the stability of the gel. The photoswitching properties of the hybrid by UV-visible light and together with the very good fatigue resistance over at least 22 cycles of photoconversion made the system very promising for light modulation material chemistry.

Acknowledgements

The authors want to thanks financial support to Ministry of Science, Technology and Productive Innovation of Argentine (Raíces Program, C. Milstein, R.E.G); National Scientific and Technical Research Council (CONICET-Argentina), University of Buenos Aires and National Agency of Scientific and Technological Promotion of Argentina (ANPCyT-Argentina), General Foundation University of Valencia (R.E.G contract).

Notes and references

1. A. P. Alivisatos, *Science*, 1996, **271**, 933-937.
2. X. Peng, L. Manna, W. Yang, J. Wickham, E. Scher, A. Kadavanich and A. P. Alivisatos, *Nature*, 2000, **404**, 59-61.
3. A. M. Smith and S. Nie, *Accounts of Chemical Research*, 2010, **43**, 190-200.
4. R. E. Galian and M. d. l. Guardia, *TrAC Trends in Analytical Chemistry*, 2009, **28**, 279-291.
5. B. A. Kairdolf, A. M. Smith, T. H. Stokes, M. D. Wang, A. N. Young and S. Nie, *Annual Review of Analytical Chemistry*, 2013, **6**, 143-162.
6. W. R. Algar, A. J. Tavares and U. J. Krull, *Analytica Chimica Acta*, 2010, **673**, 1-25.
7. M. Green, *Journal of Materials Chemistry*, 2010, **20**, 5797-5809.
8. W. J. Peveler, J. C. Bear, P. Southern and I. P. Parkin, *Chemical Communications*, 2014, **50**, 14418-14420.
9. M. Cametti and Z. Dzolic, *Chemical Communications*, 2014, **50**, 8273-8286.
10. Y. S. Zhao, H. Fu, A. Peng, Y. Ma, D. Xiao and J. Yao, *Advanced Materials*, 2008, **20**, 2859-2876.
11. Y. Wu, S. Wu, G. Zou and Q. Zhang, *Soft Matter*, 2011, **7**, 9177-9183.
12. P. D. Wadhavane, M. A. Izquierdo, F. Galindo, M. I. Burguete and S. V. Luis, *Soft Matter*, 2012, **8**, 4373-4381.
13. P. D. Wadhavane, R. E. Galian, M. A. Izquierdo, J. Aguilera-Sigalat, F. Galindo, L. Schmidt, M. I. Burguete, J. Pérez-Prieto and S. V. Luis, *Journal of the American Chemical Society*, 2012, **134**, 20554-20563.
14. V. C. Edelsztein, E. A. Jares-Erijman, K. Mullen, P. H. Di Chenna and C. C. Spagnuolo, *Journal of Materials Chemistry*, 2012, **22**, 21857-21861.
15. E. Jares-Erijman, L. Giordano, C. Spagnuolo, K. Lidke and T. M. Jovin, *Molecular Crystals and Liquid Crystals*, 2005, **430**, 257-265.
16. S. A. Díaz, G. O. Menéndez, M. H. Etchehon, L. Giordano, T. M. Jovin and E. A. Jares-Erijman, *ACS Nano*, 2011, **5**, 2795-2805.
17. L. Zhu, M.-Q. Zhu, J. K. Hurst and A. D. Q. Li, *Journal of the American Chemical Society*, 2005, **127**, 8968-8970.
18. K. Borjesson, M. Herder, L. Grubert, D. T. Duong, A. Salleo, S. Hecht, E. Orgiu and P. Samori, *Journal of Materials Chemistry C*, 2015, **3**, 4156-4161.
19. V. C. Edelsztein, G. Burton and P. H. Di Chenna, *Tetrahedron*, 2010, **66**, 2162-2167.
20. S. Kobatake, M. Yamada, T. Yamada and M. Irie, *Journal of the American Chemical Society*, 1999, **121**, 8450-8456.
21. J. R. Lakowicz, *Principles of fluorescence spectroscopy, 3rd Edition*, Springer, 2006.
22. J. Rubio, M. A. Izquierdo, M. I. Burguete, F. Galindo and S. V. Luis, *Nanoscale*, 2011, **3**, 3613-3615.
23. J. A. Kloepfer, S. E. Bradforth and J. L. Nadeau, *The Journal of Physical Chemistry B*, 2005, **109**, 9996-10003.
24. M. J. Ruedas-Rama, A. Orte, E. A. H. Hall, J. M. Alvarez-Pez and E. M. Talavera, *ChemPhysChem*, 2011, **12**, 919-929.
25. B. R. Fisher, H.-J. Eisler, N. E. Stott and M. G. Bawendi, *The Journal of Physical Chemistry B*, 2004, **108**, 143-148.
26. M. Jones, J. Nedeljkovic, R. J. Ellingson, A. J. Nozik and G. Rumbles, *The Journal of Physical Chemistry B*, 2003, **107**, 11346-11352.
27. J. Aguilera-Sigalat, V. F. Pais, A. Doménech-Carbó, U. Pischel, R. E. Galian and J. Pérez-Prieto, *The Journal of Physical Chemistry C*, 2013, **117**, 7365-7375.

View Article Online
DOI: 10.1039/C6TC02265K

28. J. Aguilera-Sigalat, S. Rocton, J. F. Sanchez-Royo, R. E. Galian and J. Perez-Prieto, *RSC Advances*, 2012, **2**, 1632-1638.
29. J. Aguilera-Sigalat, J. M. Casas-Solvas, M. C. Morant-Minana, A. Vargas-Berenguel, R. E. Galian and J. Perez-Prieto, *Chemical Communications*, 2012, **48**, 2573-2575.
30. J.-J. Yan, H. Wang, Q.-H. Zhou and Y.-Z. You, *Macromolecules*, 2011, **44**, 4306-4312.
31. Z. Erno, I. Yildiz, B. Gorodetsky, F. M. Raymo and N. R. Branda, *Photochemical & Photobiological Sciences*, 2010, **9**, 249-253.
32. A. Albini, *Photochemical & Photobiological Sciences*, 2010, **9**, 1533-1534.
33. S. A. Díaz, L. Giordano, J. C. Azcárate, T. M. Jovin and E. A. Jares-Erijman, *Journal of the American Chemical Society*, 2013, **135**, 3208-3217.
34. L. Giordano, T. M. Jovin, M. Irie and E. A. Jares-Erijman, *Journal of the American Chemical Society*, 2002, **124**, 7481-7489.

View Article Online
DOI: 10.1039/C6TC02265K

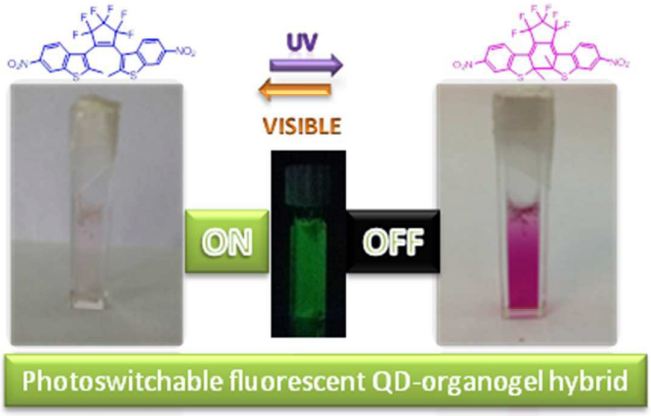

An integrated multifunctional QD-organogel hybrid with reversible photoswitchable luminescent properties is reported, combining the intrinsic properties of CdSe/ZnS core-shell QDs, a none-cholesteryl steroid organogel and a photochromic diarylethene.